Journal of Ginseng Research 46 (2022) 408–417

Contents lists available at ScienceDirect

Journal of Ginseng Research

journal homepage: https://www.sciencedirect.com/journal/journal-of-ginseng-research

Research Article

Prophylactic role of Korean Red Ginseng in astrocytic mitochondrial biogenesis through HIF-1α

Jinhong Park [a], Minjae Lee [a], Minsu Kim [a], Sunhong Moon [a], Seunghee Kim [a], Sueun Kim [a], Seong-Ho Koh [b], Young-Myeong Kim [c], Yoon Kyung Choi [a,*]

[a] Department of Bioscience and Biotechnology, Bio/Molecular Informatics Center, Konkuk University, Seoul, Republic of Korea
[b] Department of Neurology, Hanyang University Guri Hospital, Guri, Republic of Korea
[c] Department of Molecular and Cellular Biochemistry, School of Medicine, Kangwon National University, Chuncheon, Republic of Korea

ARTICLE INFO

Article history:
Received 2 March 2021
Received in revised form
1 July 2021
Accepted 7 July 2021
Available online 12 July 2021

Keywords:
Korean Red Ginseng
Astrocytic mitochondrial biogenesis
Hypoxia-inducible factor-1α
Angiogenesis
Neural stem cell differentiation

ABSTRACT

Background: Korean Red Ginseng extract (KRGE) has been used as a health supplement and herbal medicine. Astrocytes are one of the key cells in the central nervous system (CNS) and have bioenergetic potential as they stimulate mitochondrial biogenesis. They play a critical role in connecting the brain vasculature and nerves in the CNS.

Methods: Brain samples from KRGE-administered mice were tested using immunohistochemistry. Treatment of human brain astrocytes with KRGE was subjected to assays such as proliferation, cytotoxicity, Mitotracker, ATP production, and O_2 consumption rate as well as western blotting to demonstrate the expression of proteins related to mitochondria functions. The expression of hypoxia-inducible factor-1α (HIF-1α) was diminished utilizing siRNA transfection.

Results: Brain samples from KRGE-administered mice harbored an increased number of GFAP-expressing astrocytes. KRGE triggered the proliferation of astrocytes *in vitro*. Enhanced mitochondrial biogenesis induced by KRGE was detected using Mitotracker staining, ATP production, and O_2 consumption rate assays. The expression of proteins related to mitochondrial electron transport was increased in KRGE-treated astrocytes. These effects were blocked by HIF-1α knockdown. The factors secreted from KRGE-treated astrocytes were determined, revealing the expression of various cytokines and growth factors, especially those related to angiogenesis and neurogenesis. KRGE-treated astrocyte conditioned media enhanced the differentiation of adult neural stem cells into mature neurons, increasing the migration of endothelial cells, and these effects were reduced in the background of HIF-1α knockdown.

Conclusion: Our findings suggest that KRGE exhibits prophylactic potential by stimulating astrocyte mitochondrial biogenesis through HIF-1α, resulting in improved neurovascular function.

1. Introduction

The root of *Panax ginseng* is referred to as ginseng; it has been widely used in traditional medicine owing to its wide spectrum of medicinal effects. Korean Red Ginseng extract (KRGE) has been reported to be beneficial for treating CNS-associated pathophysiological conditions [1]. In the CNS, astrocytes serve different functions, such as enfolding brain microvascular endothelial cells and ensheathing synapses between neurons [2]. Healthy astrocytic mitochondria may be essential for neuronal and vascular protection as they ensure an appropriate supply of energy [3]. Glial fibrillary acidic protein (GFAP)-expressing human astrocytes are more complex and larger than their rodent counterparts and exhibit greater degree of communication with neighboring cells [4].

Following brain injury, astrocytes are reported to exhibit heme oxygenase (HO)-mediated antioxidant effects [5,6]. HO-2 is a constitutively expressed form of HO that regulates cell function. HO-1 is an inducible form of HO whose expression is transcriptionally regulated by nuclear factor erythroid 2-related factor 2 and biliverdin reductase (an enzyme that catalyzes the conversion of biliverdin to bilirubin) [7,8]. HO acts as a therapeutic modulator for inflammatory injuries, and produces carbon monoxide (CO), biliverdin, and iron by catabolizing heme [9]. CO and bilirubin can

* Corresponding author. Department of Bioscience and Biotechnology, Bio/Molecular Informatics Center, Konkuk University, Seoul, 05029, Republic of Korea.
E-mail address: ykchoi@konkuk.ac.kr (Y.K. Choi).

https://doi.org/10.1016/j.jgr.2021.07.003

induce mitochondrial biogenesis in astrocytes by activating the expression of angiogenic and metabolic factors, such as hypoxia-inducible factor-1α (HIF-1α), through the upregulation of HO-1 [10,11]. Astrocyte-derived HIF-1α protects astrocytes from glutamate toxicity [12]. However, the effect of KRGE on the expression of astrocyte-derived HIF-1α in normal conditions has not been extensively investigated.

Here, we demonstrated the function of astrocytes in the brains of mice administered KRGE. Mitotracker staining, ATP production, and O_2 consumption assays–in addition to the analysis of proteins related to the mitochondrial respiratory chain–revealed that KRGE–induced HIF-1α expression is involved in astrocytic mitochondrial biogenesis. KRGE was found to increase the secretion of various cytokines-related to neurogenesis and angiogenesis–by human astrocytes. Conditioned media from astrocytes exposed to KRGE was found to be able to trigger the migration of endothelial cells and differentiation of adult neural stem cells (NSCs) into mature neurons, and this effect was found to be mediated via astrocyte-derived HIF-1α. Thus, under physiological conditions, KRGE may enhance beneficial neurovascular functions through astrocytes.

2. Materials and methods

2.1. Materials

DMSO (Sigma Aldrich, St. Louis, MO), fetal bovine serum (FBS) (Corning, NY, USA), and Sn(IV) protoporphyrin IX dichloride (SnPP) (Frontier Scientific, Logan, UT) were bought. KRGE was obtained from the Korean Society of Ginseng (in 2018) and stored at 4 °C. Then, 0.5 g/ml stock solution prepared in filtered distilled water was aliquoted and stored with light protection at −25 °C. 20S-ginsenoside Rg3 (Rg3(S)) and 20R-ginsenoside Rg3 (Rg3(R)) (both >98% purity) were purchased from Ambo Institute (Daejeon, South Korea). 20 mM stock solution in DMSO was stored with light protection at −25 °C.

2.2. Cell culture

Primary human brain astrocytes and human brain microvascular endothelial cells (HBMECs) were acquired from the Applied Cell Biology Research Institute (Kirkland, USA). Astrocytes were cultured in Dulbecco's modified Eagle medium (DMEM, HyClone) supplemented with 10% FBS. When astrocytes reached 80% density, the media were replaced with serum-free DMEM. Cells were treated with distilled water or KRGE for 24 h in serum-free DMEM. HBMECs were grown in M199 (HyClone) supplemented with 20% FBS, 10 U/mL heparin (Sigma Aldrich), and 3 ng/mL basic fibroblast growth factor (Merck Millipore). Adult rats (aged 43-55 days) NSCs (Merck Millipore) were cultured in proliferation media (STEMCELL) on a laminin (Sigma Aldrich)-coated dish. NSCs were reached to 70% density, and cells were incubated for 4 days in differentiation medium (STEMCELL) with astrocyte conditioned media (ACM) at a 1:1 ratio.

2.3. Brain tissues and immunohistochemistry

Male C57BL/6 mice were purchased from Joong Ah Bio Inc. (Suwon, South Korea) and were maintained in standard conditions with water and food available *ad libitum*. All mouse experiments were approved by the Animal Ethics Committee of Kangwon National University (approval number KW-181109-1). Additionally, this investigation conformed to the Guide for the Care and Use of Laboratory Animals published by the United States National Institutes of Health. KRGE (0.015 mg/mL) was administrated in the drinking water for 3 days. Control mice group were administrated only water. For histological analysis, mice were anesthetized using isoflurane (1.5%) and N_2O gas, and then transcardially perfused with saline. Using optimal cutting temperature compound, the freezing brain tissues were sectioned into 20 μm sections by cryostat (HM525 NX, Thermo Fisher Scientific). The sections were incubated with 4% paraformaldehyde for 15 min and washed in phosphate buffered saline (PBS) for 3 times, then incubated with 3% bovine serum albumin for 1 h. The sections were then incubated with rabbit anti-Ki67 (1:200, abcam), mouse anti-GFAP antibody (1:300, BD Bioscience) and rat anti-CD31 (1:100, BD Biosciences) in PBST (0.1% triton X-100 in PBS) at 4°C overnight. After washing, the sections were then incubated in a mixture of both TRITC-conjugated donkey anti-rabbit IgG (1:600, Jackson ImmunoResearch) and FITC-conjugated donkey anti-mouse IgG (1:600, Jackson ImmunoResearch) for 1 h at room temperature. Between incubations, the tissues were washed with PBST (0.1% Tween-20 in PBS). The sections were visualized using mounting solution (Fluoro-Gel II with DAPI, Electron Microscopy Sciences). The stained sections were subsequently examined using an inverted phase contrast microscope (Eclipse T*i*2−U, Nikon).

2.4. Western blot analysis

Whole cell extraction buffer (10 mM HEPES, 400 mM NaCl, 0.1 mM EDTA, 5% (v/v) glycerol, 1 mM DTT, 1 mM PMSF, 1X Halt™ Protease inhibitor) or Protein Extraction Solution (RIPA) (Elpis-Biotech, South Korea) was used for cell lysis. Selected amounts of proteins from the cell lysates were combined with SDS sample buffer (Glycerol 10% (v/v), Tris-Cl pH 6.8, SDS 2% (w/v) β-mercaptoethanol 1% (v/v), bromophenol blue) and subjected to 100°C for 5 min. Then, protein samples were divided using SDS-PAGE and the PVDF membranes (Merch Millipore) were blocked in Tris-buffered saline containing 0.1% Tween 20 and 5% skim milk (BD Difco). The membranes were incubated with the primary antibodies at 4°C overnight. The primary antibodies used in this study were as follows: GFAP (1:2000, BD Biosciences), cytochrome c (Cyt c) (1:3000, BD Biosciences), HIF-1α (1:3000, BD Biosciences), HO-1 (1:3000, BD Biosciences), doublecortin (DCX, 1:1000, SantaCruz Biotechnology), GAP43 (1:2000, SantaCruz Biotechnology), cytochrome c oxidase subunit (MTCO) 2 (1:1000, SantaCruz Biotechnology), VEGF (1:1000, SantaCruz Biotechnology), NeuN (1:2000, Merck Millipore), Angiogenin (1:1000, abcam), a total OXPHOS antibody cocktail (1:3000, abcam), PSD95 (1:2000, abcam), β-Actin (1:8000, Sigma Aldrich). After washing, the membranes were incubated with peroxidase-conjugated secondary antibodies (1:8000, Thermo Fisher Scientific) and visualized using enhanced ECL (Elpis-Biotech, South Korea) by using appropriate detection equipment (Fusion Solo-Vilber Lourmat, France).

2.5. Immunocytochemistry

Adult rat NSCs were cultured in 12-well plates (Corning Costar). After the NSCs reached 70% confluency, they were incubated for 4 days in differentiation medium with ACM (1:1 ratio). Media were removed, and cells were fixed in 4% paraformaldehyde for 10 min. Then, the cells were washed with 0.1% → 0.2% → 0.1% (vol/vol) Tween 20 in PBS for 10 min, following which, the cells were blocked

in 3% bovine serum albumin prepared in PBST (PBS containing 0.1% Triton X-100) for 1 h at room temperature. Cells were then incubated overnight with mouse anti-DCX (1:300, ThermoFisher Scientific) and rabbit anti-PSD95 (1:300, Abcam) antibodies prepared in PBST (at 4°C). The subsequent procedures and secondary antibody concentrations were identical to those used for immunohistochemistry. Images were captured using a fluorescent microscope (Eclipse Ti2–U, Nikon).

2.6. Cell proliferation (cell counting kit-8 (CCK-8)) assay

Human astrocytes were cultured in 12-well plates (Corning Costar). Astrocytes were reached to 80% confluence and then treated with distilled water or KRGE for 23 h in 0% FBS DMEM. CCK-8 (30 μL, Dojindo) was added to astrocytes at 37°C for 1 h. A plate reader (Epoch Microplate Spectrophotometer, BioTek) was utilized to determine the absorbance at a wavelength of 450 nm. The backdrop signal was measured at 630 nm and was subtracted from the absorbance detected at 450 nm.

2.7. Cytotoxicity (lactate dehydrogenase (LDH)) assay

Astrocyte media were obtained from the 12-well plate, and then were centrifuged for 5 min at 7,000 rpm. The 50 μL supernatants were relocated to a 96-well plate (CM) in triplicates. The 50 μL medium without cells was used as the CM blank for that condition. Astrocytes were washed with PBS two times and added with 500 μL of 5% triton X-100 (Sigma Aldrich) in PBS at 37°C for 20 min. Lysed cells were centrifuged for 5 min at 15,000 rpm. The 50 μL supernatant was moved to a 96-well plate (WCL) in triplicates. The 50 μL supernatant without cells was utilized to serve as the WCL blank for that condition. Using an LDH assay kit (Takara), the dye solution was mixed with the catalyst at a 45:1 ratio. The mixed detection kit reagent (50 μL) was included to each of 96 wells of the plate used for the assay rapidly after the supernatant. The assay plates were located at room temperature in the dark for 20 minutes, and then they were read utilizing a standard plate reader (Epoch Microplate Spectrophotometer, BioTek) and a reference wavelength of 490 nm.

$$\text{Cytotoxicity (\%)} = (\text{CM value} - \text{CM blank})/ (\text{WCL value} - \text{WCL blank}) + (\text{CM value} - \text{CM blank})) \times 100$$

2.8. Transfection

Astrocytes were reached to 70% confluence and transiently transfected with pcDNA3.1/HIF-1α (provided by Dr. Gregg L. Semenza, The Johns Hopkins University) and HO-1 siRNA (50 nM) using Lipofectamine and Plus reagent (Thermo Fisher Scientific). Human astrocytes were transfected with 50 nM control or HIF-1α siRNA using RNAiMax (Thermo Fisher Scientific). After 12 h of recovery, the cells were treated with or without 0.5 mg/mL KRGE for 24 h in serum-free DMEM. The siRNAs pointing human HIF-1α were purchased from Dharmacon (Lafayette, USA). Other commercial human siRNAs used for the control and HO-1 were bought from Santa Cruz Biotechnology (Dallas, USA).

2.9. Conditioned media from astrocytes (ACM) preparation

When human astrocytes reached 80% density, the medium was changed to serum-free DMEM. Then, the cells were treated with distilled water or KRGE for 24 h, and conditioned media from astrocytes (ACM) were collected. After centrifugation at 1,500 rpm for 5 min to remove cell debris, ACM were used for the migration, cytokine array, and NSC differentiation assays. For the NSC differentiation assay, NSCs were nurtured with ACM and differentiation media at a 1:1 ratio for 4 days. For the migration assay, HBMECs were incubated with ACM for 4 h.

2.10. Human XL cytokine array

Factors secreted from astrocytes exposed to KRGE were evaluated using Human XL Cytokine Array Coordinates (R&D systems). Media were concentrated using Amicon ultra-4 centrifugal filter (Millipore, 3-kDa cutoff). Then, concentrated ACM were subjected to Human XL Cytokine Array, according to manufacturer's instructions. We quantified the intensity of dots using imageJ. Control group was set to "1" and relative intensity was analyzed.

2.11. Mitochondrial biogenesis assay

Intracellular active mitochondria levels were assessed using quantitative fluorescence imaging by using the mitochondria-sensitive dye Mitotracker (Thermo Fisher Scientific, Waltham, MA). Astrocytes plated on 18 mm round coverslips in 12-well plates were cultured to 80% density. Cells were subjected to distilled water or KRGE for 23.5 h. Cells were treated with 0.5 μM Mitotracker for further 30 min. After washing with PBS, fluorescent images of live cells were acquired using an inverted phase contrast microscope (Eclipse Ti2–U, Nikon).

2.12. O_2 consumption

Real time O_2 consumption was assessed by the O_2 Consumption Rate Assay Kit (Cayman, Ann Arbor, USA). 80% confluent astrocytes were incubated in regular 96-well plates with distilled water or KRGE for 24 h in serum-free DMEM media, and 10 μL of an O_2 sensor probe were included to each well. After covering the wells with Mineral Oil, the plates were calculated using a filter combination and emission and excitation wavelengths of 650 and 380 nm, respectively, at 37°C (BioTek, Winooski, USA).

2.13. ATP assay

The cellular ATP amounts were detected by an ATP colorimetric assay kit (BioVision, Milpitas, CA) according to the manufacturer's instructions. 80% confluent astrocytes were treated with distilled water or KRGE in serum-free DMEM media for 24 h, and then lysed in 120 μL of ATP assay buffer and centrifuged at 15,000 × *g* for 3 min at 4°C. The collected 50 μL supernatant was combined with 50 μL of reaction mixture reagents and the plates were located at room temperature for 1 h while being protected from light and the absorbance was measured at 570 nm using a colorimetric assay reader (Epoch Microplate Spectrophotometer, BioTek). Lysed cells were quantified using BCA (ThermoFisher Scientific). Then, ATP levels/proteins in control group (0 mg/ml KRGE) was set to "1", and KRGE-treated groups are adjusted to the control group.

2.14. Cell migration assay

For the Transwell migration assay, ACM were prepared and concentrated (× 2) using a centrifugal filter device (3 kDa cut-off,

Merck Millipore). The chemotactic motility of HBMECs was measured utilizing Transwell plates (8.0 μm pore size, 6.5 mm of diameter, Corning Costar). The lower surface of Transwell plates was coated with gelatin (10 μg). HBMECs (1×10^5 cells) were loaded onto the upper well. After 4 h of incubation, the migrated cells were fixed with methanol and stained with hematoxylin for 5 min and subsequently with eosin for 1 min. The migratory cells were observed by using an inverted phase contrast microscope (IX71, Olympus).

2.15. Data analysis

Quantification of the intensity of the protein band, which was achieved using western blot experiments, was evaluated using ImageJ (http://rsb.info.nih.gov/ij/) program. In this study, GraphPad Prism 6 was utilized for overall statistical analysis. Multiple comparisons were evaluated using One-way ANOVA plus Tukey's test (mean ± SD). A $P < 0.05$ was regarded statistically significant. $^*P < 0.05$; $^{**}P < 0.01$; $^{***}P < 0.001$.

3. Results

3.1. KRGE increases the proportion of GFAP-positive astrocytes in the subventricular zone (SVZ) in normal mice

To determine the effects of KRGE on astrocytic functions, normal mice were administered KRGE for 3 days via drinking water, and the expression of GFAP and Ki67 (a cell proliferation marker) was examined. We focused on the SVZ because in mice, adult neurogenesis occurs in that region [13] (Fig. 1A–C). KRGE administration resulted in an increase in the proportion of both GFAP- and Ki67-positive cells in the mouse SVZs compared with the control mice (Fig. 1B), showing close localization (Fig. 1C). This result was confirmed using western blotting, which showed that GFAP expression was upregulated in the SVZs of mouse brains (Fig. 1D). As KRGE-induced increase in the proportion of astrocytes closely associated with Ki67 immunofluorescence (Fig. 1B–C), we examined the proliferation of astrocytes at various KRGE concentrations. When the cells were treated with 0.25 and 0.5 mg/mL KRGE, significant increases in cellular proliferation were detected (Fig. 1E) without cell toxicity (Fig. 1F). These data demonstrate that KRGE may induce astrocyte proliferation both *in vivo* and *in vitro*.

3.2. KRGE increases the proportion of active mitochondria and activates the HO-1-HIF-1α axis in human astrocytes

We hypothesized that active mitochondria might be responsible for astrocyte proliferation in KRGE-treated conditions. When astrocytes were subjected to various assays, such as Mitotracker staining (Fig. 2A), ATP production (Fig. 2B), and oxygen consumption rate (Figs. 2C), 0.5 mg/mL KRGE significantly increased all the parameters tested, revealing active mitochondrial functions (Fig. 2A–C). Increased oxygen consumption in the mitochondria can induce intracellular hypoxia [11]. Thus, we detected HIF-1α protein expression in KRGE-treated astrocytes. KRGE (0.5 mg/mL) markedly increased the HIF-1α protein levels (Fig. 2D). Similar to that of HIF-1α, the expression of HO-1 was increased in KRGE-treated astrocytes in a concentration-dependent manner (Fig. 2E). We also tested the role of the ginsenoside (saponin monomer), Rg3, with respect to the expression of HIF-1α and HO-1 (Supplementary

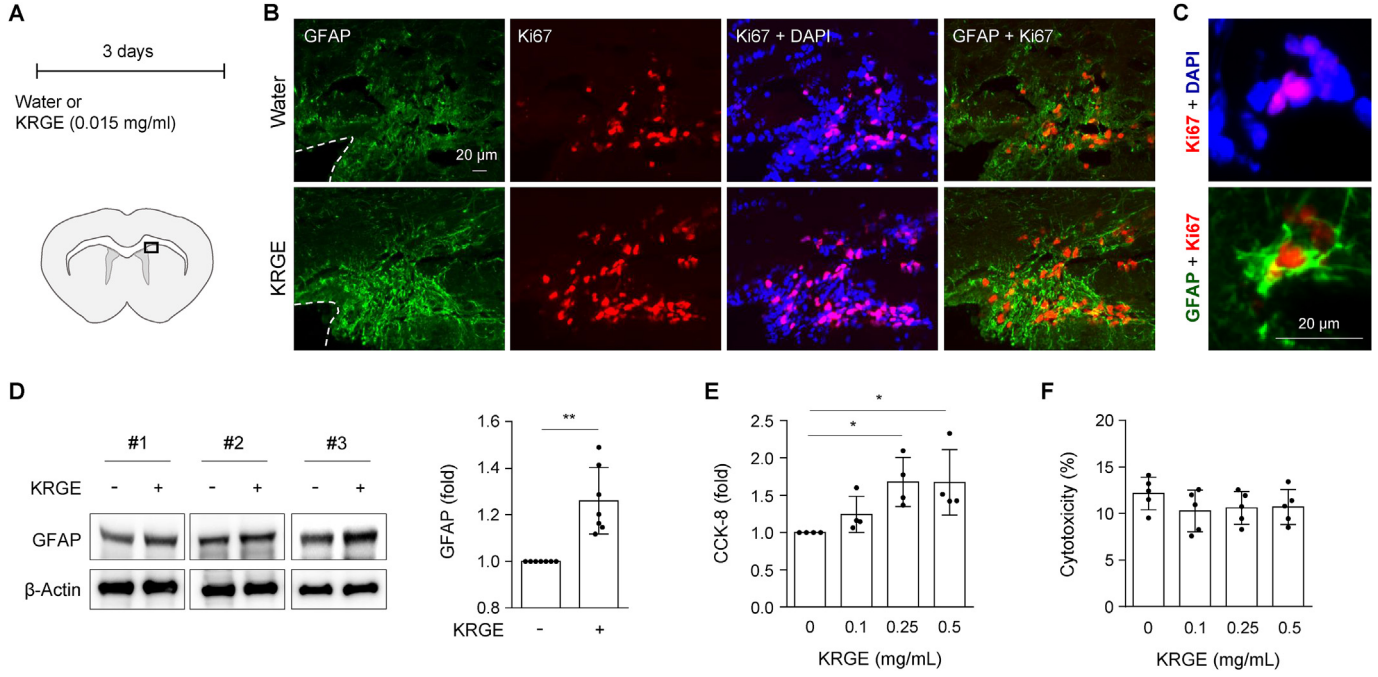

Fig. 1. KRGE induces GFAP-positive astrocytes in the subventricular zone in normal mice. (A, upper) Mice (8-week-old young adult) were subjected to 0.015 mg/mL KRGE via drinking water for 3 days. Control mice were only administered drinking water for 3 days. (A, lower) The subventricular zone (SVZ) was detected at bregma 1.5. (B–C) Fluorescence micrographs of mouse SVZ illustrates the localization of GFAP (green), Ki67 (red) and DAPI (blue) ($N = 4$). Scale bars = 20 μm. (D) Western blots of GFAP ($N = 7$) in mice brains are shown (left) as well as a quantitative graph (right). $^{**}P < 0.01$ (paired t-test). (E) Astrocyte proliferation activity was evaluated using a CCK-8 cell counting kit. KRGE-treatment groups indicated by the labeling concentration on the x-axis ($N = 4$). (F) Cytotoxicity of astrocytes was detected using an LDH assay. KRGE-treatment groups indicated by the labeling concentration on the x-axis ($N = 5$).

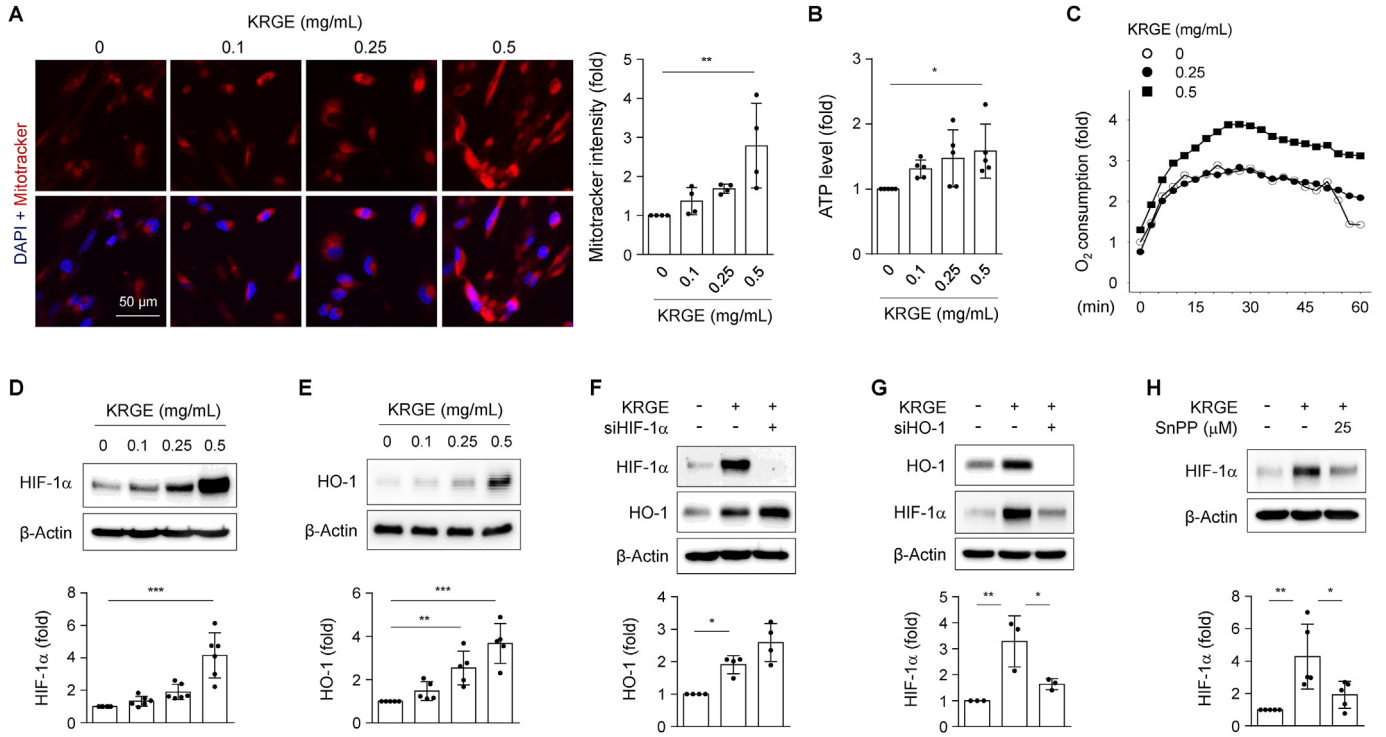

Fig. 2. KRGE induces intracellular active mitochondria and HO-1-HIF-1α axis in human astrocytes. Mitochondrial biogenesis was determined by staining with Mitotracker (left), and its intensity was quantified ($N = 4$). The average intensity was obtained from random five cells from each image (× 20). (B) Relative ATP levels/proteins are shown ($N = 5$). (C) Mitochondrial oxygen consumption was detected ($N = 3$). (D-E) Astrocytes were treated with the indicated concentration of KRGE for 24 h. Western blots of HIF-1α and HO-1 are shown (upper), and quantitative graphs are demonstrated (lower). (F-G) Astrocytes were transfected with HIF-1α siRNA (si−HIF−1α) or si−HO−1 and the indicated protein levels were evaluated using western blots. Control siRNA (si-control) was used for the control group. (H) Astrocytes were pretreated with 25 μM SnPP for 10 min, then 0.5 mg/mL KRGE was added for 24 h. Western blots of HIF-1α (upper), and a quantitative graph are shown (lower) ($N = 4$).

Fig. 1A and B) because 20S-ginsenoside Rg3 (Rg3(S)) plays a beneficial role in endothelial cell survival during serum deprivation [14] and in neuroprotection after ischemic stroke in a rat model [15]. Increased protein levels were detected in Rg3(S)-treated cells (Supplementary Fig. 1A and B), while Rg3(R) treatment did not induce an increase in HO-1 levels (Supplementary Figure 1C).

To elucidate the relationship between HIF-1α and HO-1 expression under conditions of KRGE (0.5 mg/mL) treatment, human astrocytes were transfected with siHIF-1α (Fig. 2F) and siHO-1 (Fig. 2G). Further, we evaluated HIF-1α expression when HO activity was blocked in cells following SnPP treatment (Fig. 2H). Our results demonstrated that HO-1 was an upstream signal for HIF-1α because HIF-1α knockdown did not result in reduced HO-1 expression (Fig. 2F), while the inhibition of HO-1 expression markedly reduced the HIF-1α protein levels under conditions of KRGE treatment (Fig. 2G–H). These results imply that KRGE increases mitochondrial activity in astrocytes, possibly inducing intracellular hypoxia and the consequent stabilization of the HO-1-HIF-1α pathway. Rg3(S) may be one of the ginsenosides involved in the HO-1-HIF-1α signaling pathway in astrocytes.

3.3. *KRGE promotes astrocytic mitochondrial biogenesis in a HO-1-HIF-1α axis-dependent manner*

Active mitochondrial biogenesis results in the upregulation of mitochondrial proteins (i.e., MTCO1 and MTCO2) and related nuclear proteins (i.e., cytochrome c (Cyt c)). ATP is produced in the mitochondria during oxidative phosphorylation. Oxidative phosphorylation complexes (I-IV) are multi-subunit enzymes that function along with ATP synthase (complex V) [16]. The expression of oxidative phosphorylation complexes increased with the increasing concentrations of KRGE; for example, complex I (CI) levels were significantly increased in response to KRGE treatment (Supplementary Figure 2A). The expression of Cyt c was similar to that of CI, as evidenced by increased levels in KRGE-treated cells (Supplementary Figure 2B). Further, 0.5 mg/mL KRGE upregulated the expression of MTCO2 (Supplementary Figure 2C). The KRGE-mediated upregulation of oxidative phosphorylation complexes, Cyt c, and MTCO2, was blocked by the HO inhibitor SnPP (Fig. 3A–C). KRGE-mediated upregulation of MTCO2 was decreased in the background of HO-1 knockdown (Fig. 3D). These results suggest that KRGE-mediated HO-1 is involved in the regulation of mitochondrial functions in astrocytes. Then, we examined whether HO-1-dependent mitochondrial biogenesis was mediated via the HIF-1α signaling pathway. HO-1 expression was knocked down using siHO-1, and HIF-1α was overexpressed using the HIF-1α-activating vector. HIF-1α overexpression restored MTCO2 expression, even under conditions of HO-1 knockdown (Fig. 3E and Supplementary Figure 3), indicating that HIF-1α may play a key role in KRGE-induced mitochondrial biogenesis. To confirm the effects of HIF-1α on mitochondrial biogenesis in astrocytes, we used the approach of HIF-1α knockdown. When HIF-1α was knocked down

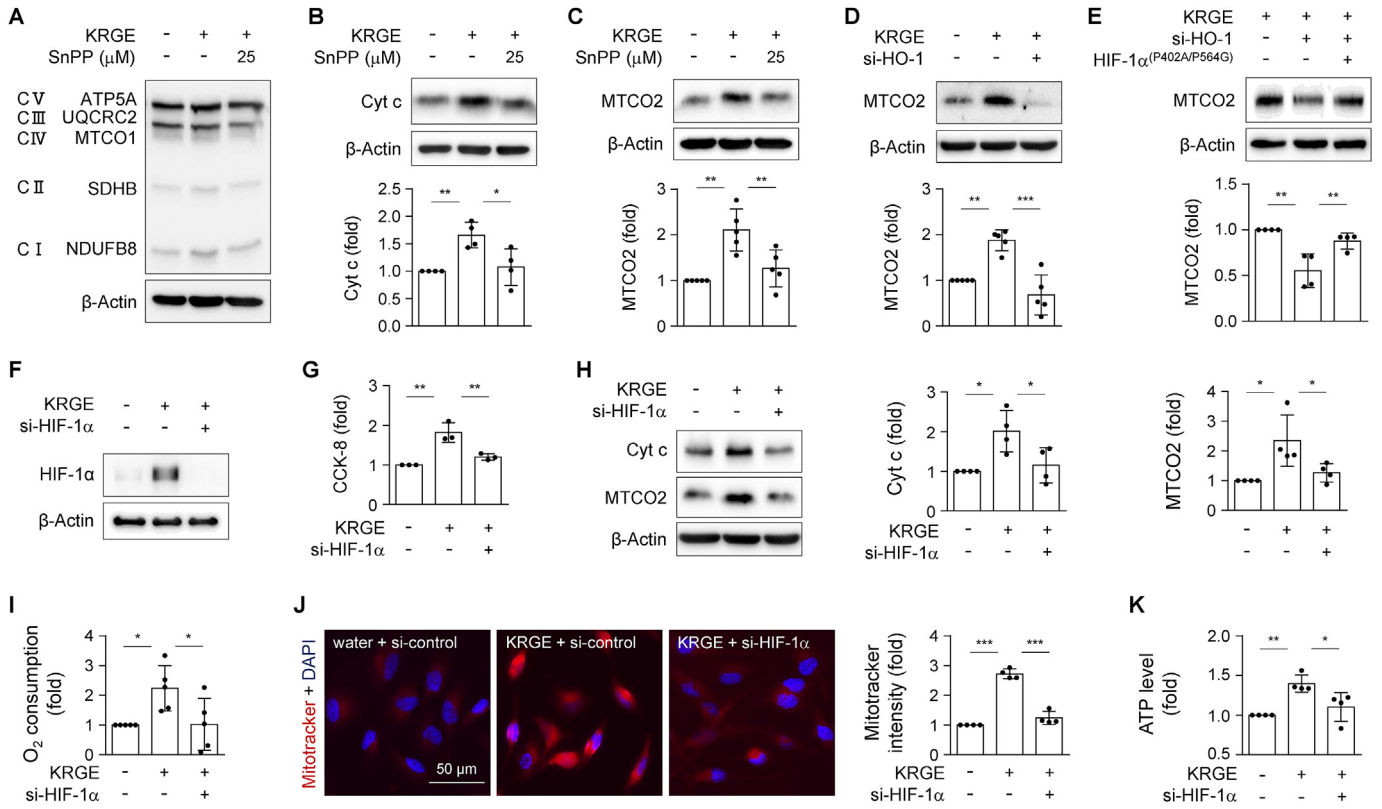

Fig. 3. KRGE promotes astrocytic mitochondrial biogenesis in an HO-1-HIF-1α axis-dependent manner. (A-C) Oxidative phosphorylation complexes were detected using western blots when human astrocytes were pretreated with or without 25 μM SnPP for 10 min, followed by 0.5 mg/mL KRGE treatment for 24 h (A). Cyt c ($N = 4$) and MTCO2 ($N = 5$) were detected using western blots (B–C). (D) Human astrocytes were transfected with si–HO–1 and the MTCO2 protein levels were evaluated using western blots ($N = 5$). (E) Astrocytes were transfected with si–HO–1 and HIF-1α$^{(P402A/P564G)}$ overexpressing vector, and the MTCO2 protein levels were assessed using western blots ($N = 4$). (F) Astrocytes were transfected with si–HIF–1α and the HIF-1α protein levels were evaluated using western blots. (G) Astrocytes were transfected with si–HIF–1α and a CCK-8 assay was used to analyze cell proliferation ($N = 3$). (H) Astrocytes were transfected with si–HIF–1α and the protein levels were evaluated using western blots. (I) Mitochondrial oxygen consumption was detected using the Oxygen Consumption Rate Assay Kit. A quantitative graph was drawn by analyzing the 15 min values ($N = 4$). (J) Mitochondrial biogenesis was determined by staining with Mitotracker ($N = 4$). The average intensity was obtained from five random cells from each image (× 20). (K) Relative ATP levels/proteins are shown ($N = 4$).

in background of KRGE treatment (Fig. 3F), cell proliferation was reduced (Fig. 3G), and the expression of Cyt c and MTCO2 was decreased (Fig. 3H). Moreover, HIF-1α knockdown resulted in reduced KRGE-induced oxygen consumption (Fig. 3I), Mitotracker intensity (Fig. 3J), and ATP levels (Fig. 3K), thereby confirming the role of HIF-1α in KRGE-induced mitochondrial functions. Thus, KRGE enhances astrocytic mitochondrial biogenesis via HIF-1α upregulation.

3.4. Astrocyte-derived HIF-1α controls the release of various cytokines involved in regeneration

KRGE-treated astrocytes communicate with the surrounding cells in neurovascular systems [2]. Therefore, we investigated the ACM for the presence of secreted factors using a human cytokine array kit (Fig. 5A). We tested the ACM obtained from KRGE-treated cells (both control and HIF-1α knockdown conditions) (Fig. 4A). KRGE enhanced the secretion of angiogenin, epithelial-neutrophil activating peptide (ENA-78), growth-regulated oncogene α (GROα), interleukin-17A (IL-17A), stromal-derived factor-1α (SDF-1α) and VEGF, and these effects were blocked upon the downregulation of HIF-1α in astrocytes (Fig. 4B). The reference spot was unchanged in all groups (Fig. 4C). To confirm these results, we examined the expression of angiogenin and VEGF in astrocytes. Similar to the secretion pattern, the upregulation of angiogenin and VEGF in KRGE-treated astrocytes was inhibited upon knocking down HIF-1α (Fig. 4D–E). Considering that HIF-1α regulates astrocytic metabolism and glycolysis [17], HIF-1α-mediated secretion of various cytokines and growth factors may further contribute to neurovascular functions as well as astrocytic mitochondrial biogenesis.

3.5. KRGE-treated astrocytes regulate the differentiation of adult NSCs into mature neurons through astrocytic HIF-1α

To determine the interactions between astrocytes and NSCs, we tested the effects of KRGE-treated ACM on the differentiation of adult NSCs. For probing the human brain, it would be beneficial to obtain human adult NSCs. However, it is difficult to obtain human adult NSCs. Therefore, researchers have used adult rodent NSCs [18,19]. We also examined the effects of direct treatment with KRGE on adult rat NSCs (Fig. 5A–B). Direct treatment with KRGE did not

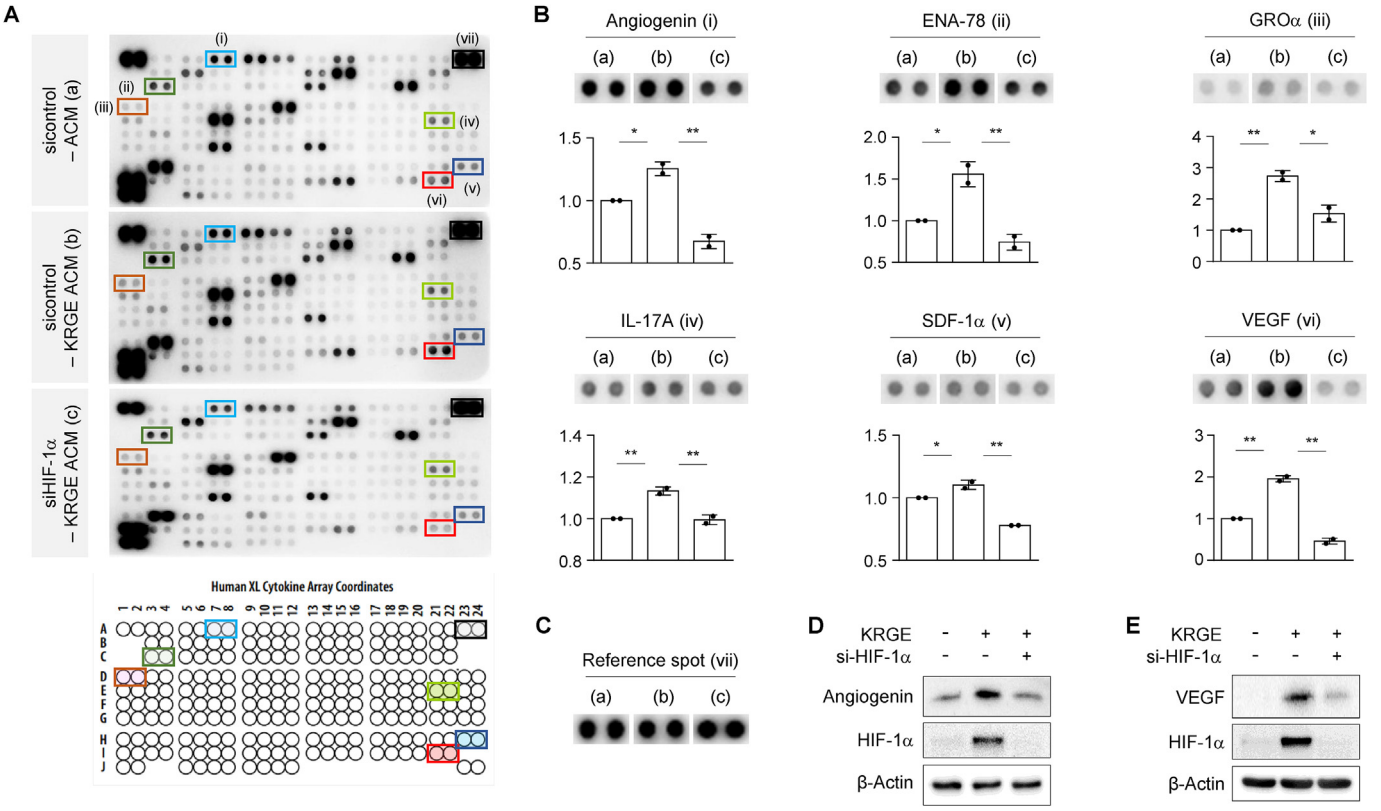

Fig. 4. Astrocyte-derived HIF-1α controls the release of various cytokines involved in the regeneration from KRGE-treated cells. (A-C) Astrocytes were transfected with si-control or si–HIF–1α, then treated with 0.5 mg/mL KRGE for 24 h. ACM were subjected to Human XL Cytokine Array. (D-E) Astrocytes were transfected with si-control or si–HIF–1α, then treated with 0.5 mg/mL KRGE for 24 h. Angiogenin and VEGF protein levels were detected using western blots ($N = 3$).

affect the expression of neuronal markers, i.e., DCX, GAP43, NeuN, and PSD95 when NSCs were differentiated for 4 days (Fig. 5B). In contrast, KRGE-treated ACM significantly promoted the neuronal differentiation of adult NSCs (Fig. 5C–D) and axon branching [20] detected by PSD95 and DCX (Fig. 5E), and these effects were blocked when ACM were obtained under HIF-1α-knockdown conditions (Fig. 5E–G). Next, we found that ACM significantly enhanced NSC proliferation and reduced NSC cytotoxicity (compared with control media; "no cell") (Supplementary Fig. 4A and B). The factors secreted from astrocytes promoted NSC proliferation and reduced cytotoxicity, but these effects were not altered upon treating the CM from astrocytes with KRGE. However, KRGE-treated astrocytes induced a substantial increase in the neuronal differentiation of NSCs, and a crosstalk between astrocytes and neural stem cells was responsible for this phenomenon.

3.6. KRGE-treated astrocytes upregulate the migration of microvascular endothelial cells through astrocytic HIF-1α

Immunoreactivity of CD31 (endothelial cell marker) was not overlap with Ki67 immunoreactivity in SVZ (Supplementary Figure 5). Since KRGE-administered mouse brains display the increased association between GFAP-positive astrocytes and CD31-positive endothelial cells compared with control mouse brains (Fig. 6A), the angiogenic capacity was tested in KRGE-treated ACM using an endothelial cell migration assay (a well-known *in vitro* angiogenic assay) [21]. We collected KRGE-treated ACM and concentrated them twice (Fig. 6B). Treatment of HBMECs with KRGE-ACM facilitated endothelial cell migration in a concentration-dependent manner (Fig. 6C), and these effects were abolished by ACM obtained from HIF-1α knockdown KRGE-treated astrocytes (Fig. 6D). We found that KRGE promoted astrocyte functions by enhancing the angiogenic capacity.

4. Discussion

Here, we demonstrated that KRGE induces astrocytic mitochondrial biogenesis by upregulating HIF-1α, a master regulator of the cellular response to hypoxia; this transcription factor is stabilized and activated by hypoxia [22]. In this study, the expression of astrocytic HIF-1α was induced by KRGE under normoxic conditions, and this effect was in turn induced by HO-1. Activation of the HO-1-HIF-1α axis can be observed under normal O_2 tension conditions. In our previous study, we had demonstrated that HO metabolites, such as CO, affected the synthesis and stability of HIF-1α in human astrocytes [11,23]. Therefore, we hypothesized that KRGE-induced HO-1 produces CO, consequently inducing an upregulation of HIF-1α expression. Overexpression of active HIF-1α (HIF-1α$^{(P402A/P564G)}$) in the background of KRGE treatment induces the upregulation of MTCO2, even in HO-1-knockdown conditions, implying that HIF-1α expression plays a role in astrocytic mitochondrial functions. The proline residues 402 and 564 in HIF-1α coordinately

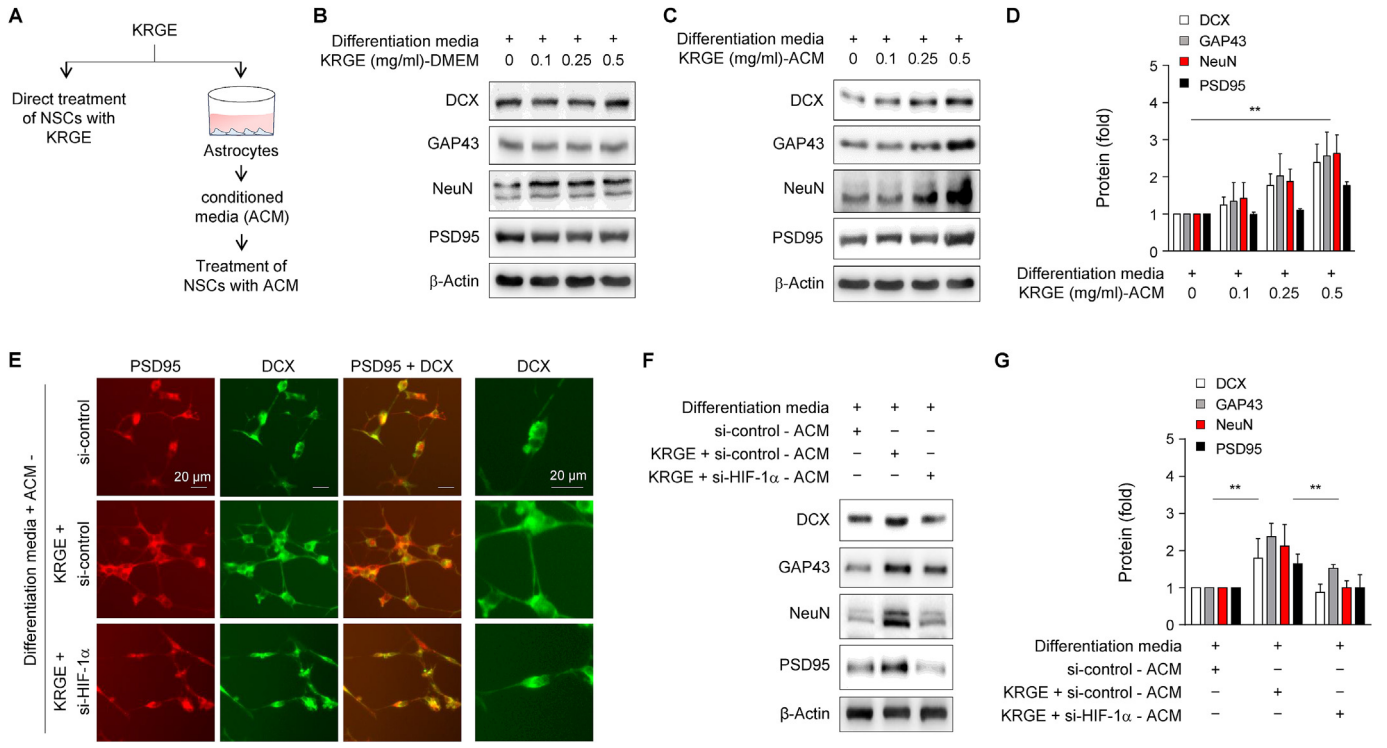

Fig. 5. KRGE-treated astrocytes regulate adult neural stem cell differentiation to mature neurons through astrocytic HIF-1α. (A) Schematic figure showing the experimental procedures. (B) NSCs were incubated with DMEM containing the indicated concentrations of KRGE. Then, differentiation medium was added, and incubated for 4 days. The indicated protein levels were evaluated using western blots ($N = 3$). (C-D) NSCs were incubated with KRGE-treated ACM and differentiation media at a 1:1 ratio for 4 days, and the protein levels of DCX ($N = 5$), GAP43 ($N = 3$), NeuN ($N = 3$), and PSD95 ($N = 5$) were evaluated using western blots. (E-G) NSCs were incubated with KRGE-treated si-control or si−HIF−1α ACM and differentiation media at a 1:1 ratio for 4 days. (E) Fluorescence micrographs of adult rat NSCs illustrates the expression of PSD95 (red) and DCX (green) ($N = 5$). Scale bars = 20 μm. (F-G) The protein levels of DCX ($N = 5$), GAP43 ($N = 5$), NeuN ($N = 4$), and PSD95 ($N = 3$) were evaluated using western blots.

regulate its hydroxylation via prolyl hydroxylase domains (PHDs), which require O_2 as a substate [24]. As intracellular O_2 levels are decreased in response to increased mitochondrial biogenesis, HIF-1α can be stabilized as a result of the inhibition of O_2 utilization by PHDs [11], a phenomenon that blocks HIF-1α degradation through a proteasome pathway [25].

ATP is produced in the mitochondria during oxidative phosphorylation through oxidative phosphorylation complexes. An electron transfer between the complexes occurs, which is mediated by two small components, i.e., lipid-soluble ubiquinone and water-soluble cytochrome c (Cyt c). They diffuse between the respiratory complexes I and III and III and IV, respectively (Reviewed in [16]). NADH:ubiquinone oxidoreductase subunit B8 (NDUFB8) forms oxidative phosphorylation CI. Mitochondrial membrane ATP synthase (complex V) generates ATP from ADP in the presence of a proton gradient across the mitochondrial membrane, which is generated by oxidative phosphorylation through CI to CIV. Our study shows that KRGE upregulates the protein levels of NDUFB8, MTCO2, and Cyt c as well as ATP production in astrocytes. KRGE also enhances mitochondrial biogenesis, as detected using a Mitotracker assay. These increases are inhibited by reduced HIF-1α expression, suggesting that KRGE-induced HIF-1α is involved in astrocytic mitochondrial functions.

Since astrocytes bridge neurovascular systems, KRGE-mediated astrocytic mitochondrial biogenesis may affect neuronal and vascular systems, possibly through various factors related to neurogenesis and angiogenesis. Using a cytokine array system, we found that the secreted factors were regulated by HIF-1α in KRGE-treated astrocytes. KRGE upregulated the secretion levels of angiogenin, ENA-78, GROα, IL-17A, SDF-1α, and VEGF, and these effects were blocked upon HIF-1α knockdown. The aforementioned factors are regenerative signaling molecules involved in angiogenesis and neurogenesis [26–33]. Adult neurogenesis in the SVZ and dentate gyrus is characterized by NSC proliferation, migration, and differentiation [34]. KRGE administration enhanced astrocyte proliferation in the SVZ of mouse brains under physiological conditions. Additionally, KRGE-treated astrocytes exhibited enhanced proliferation *in vitro*. As ACM significantly increased NSC proliferation and reduced NSC cytotoxicity compared with CM, and ACM from KRGE-treated cells did not affect NSC proliferation and cytotoxicity compared with ACM, we assume that KRGE may indirectly affect NSC proliferation and cytotoxicity by enhancing astrocyte proliferation.

The combined effects of secreting factors induced by KRGE on astrocytes *in vitro* possibly contribute to enhanced cell-cell communication, as evidenced by increased endothelial cell migration and adult NSC differentiation (Fig. 6E). KRGE-ACM strongly stimulates the differentiation of NSCs into mature neurons and endothelial cell migration (Fig. 6E). KRGE-mediated HIF-1α stabilization in astrocytes plays a critical role in these regenerative effects. Our novel findings suggest that KRGE-induced HIF-1α stabilization in astrocytes may have regenerative potential as this approach can be used an intervention for energy-demanding brains. We assume that KRGE-treated astrocytes may accelerate and improve the communication of cells with the microvasculature and lead to the generation of numerous synapses, even in normal brains.

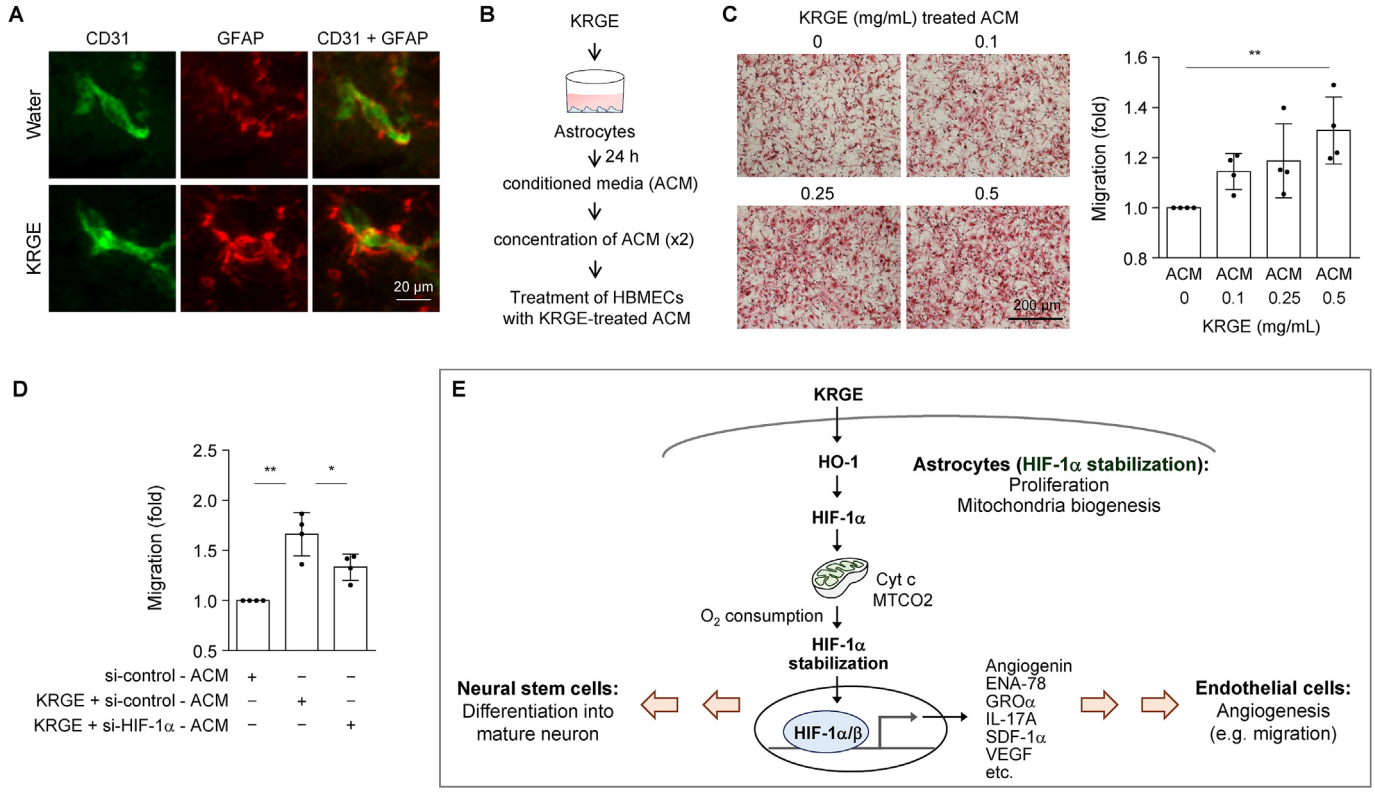

Fig. 6. KRGE-treated astrocytes upregulate the migration of microvascular endothelial cells through astrocytic HIF-1α. (A) Fluorescence micrographs of mouse SVZ illustrates the localization of CD31 (green) and GFAP (red) ($N = 3$). Scale bars = 20 μm. (B) Schematic figure showing the experimental procedures. ACM were collected when human astrocytes were incubated with KRGE for 24 h. (C) HBMECs (1×10^5) were incubated with the indicated concentrations of KRGE-treated ACM for 4 h. (D) Treatment of HBMECs with the si–HIF–1α transfection plus KRGE were tested. (C-D) A migration assay was conducted ($N = 4$). Quantitative graphs were drawn by counting the migrated cells. (E) Schematic figure showing the role of astrocytic HIF-1α in mitochondrial biogenesis and the consequent neuronal differentiation and *in vitro* angiogenesis detected based on endothelial cell migration.

Acknowledgements

Active form of HIF-1α overexpressing vector (pcDNA3.1/HIF-$1\alpha^{P402A/P564G}$) was thankfully provided by Dr. Gregg L. Semenza (Johns Hopkins University, USA).

Appendix A. Supplementary data

Supplementary data to this article can be found online at https://doi.org/10.1016/j.jgr.2021.07.003.

Funding

This study was supported by the 2018 & 2019 grant from the Korean Society of Ginseng. This work was supported by the National Research Foundation of Korea (NRF) grant funded by the Korea Government (MSIT) (2020R1A2C1004397). This research was also supported by a grant of the Korea Health Technology R&D Project through the Korea Health Industry Development Institute (KHIDI), funded by the Ministry of Health & Welfare, Republic of Korea (HI20C0253).

References

[1] Kim HJ, Kim P, Shin CY. A comprehensive review of the therapeutic and pharmacological effects of ginseng and ginsenosides in central nervous system. J Ginseng Res 2013;37(1):8–29. https://doi.org/10.5142/jgr.2013.37.8.
[2] Abbott NJ, Ronnback L, Hansson E. Astrocyte-endothelial interactions at the blood-brain barrier. Nature Reviews Neuroscience 2006;7(1):41–53.
[3] Hayakawa K, Esposito E, Wang X, Terasaki Y, Liu Y, Xing C, et al. Transfer of mitochondria from astrocytes to neurons after stroke. Nature 2016;535(7613):551–5. https://doi.org/10.1038/nature18928.
[4] Oberheim NA, Takano T, Han X, He W, Lin JH, Wang F, et al. Uniquely hominid features of adult human astrocytes. J Neurosci 2009;29(10):3276–87. https://doi.org/10.1523/JNEUROSCI.4707-08.
[5] Hettiarachchi NT, Boyle JP, Dallas ML, Al-Owais MM, Scragg JL, Peers C. Heme oxygenase-1 derived carbon monoxide suppresses Abeta1-42 toxicity in astrocytes. Cell Death Dis 2017;8(6):e2884. https://doi.org/10.1038/cddis.2017.276.
[6] Chen-Roetling J, Benvenisti-Zarom L, Regan RF. Cultured astrocytes from heme oxygenase-1 knockout mice are more vulnerable to heme-mediated oxidative injury. J Neurosci Res 2005;82(6):802–10. https://doi.org/10.1002/jnr.20681.
[7] Lee BS, Heo J, Kim YM, Shim SM, Pae HO, Chung HT. Carbon monoxide mediates heme oxygenase 1 induction via Nrf2 activation in hepatoma cells. Biochem Biophys Res Commun 2006;343(3):965–72.
[8] Tudor C, Lerner-Marmarosh N, Engelborghs Y, Gibbs PE, Maines MD. Biliverdin reductase is a transporter of haem into the nucleus and is essential for regulation of HO-1 gene expression by haematin. Biochem J 2008;413(3):405–16. https://doi.org/10.1042/BJ20080018.
[9] Ryter SW, Choi AM. Targeting heme oxygenase-1 and carbon monoxide for therapeutic modulation of inflammation. Transl Res 2016;167(1):7–34. https://doi.org/10.1016/j.trsl.2015.06.011.
[10] Choi YK, Park JH, Baek YY, Won MH, Jeoung D, Lee H, et al. Carbon monoxide stimulates astrocytic mitochondrial biogenesis via L-type Ca2+ channel-mediated PGC-1alpha/ERRalpha activation. Biochem Biophys Res Commun 2016;479(2):297–304. https://doi.org/10.1016/j.bbrc.2016.09.063.
[11] Choi YK, Park JH, Yun JA, Cha JH, Kim Y, Won MH, et al. Heme oxygenase metabolites improve astrocytic mitochondrial function via a Ca2+-dependent HIF-1alpha/ERRalpha circuit. PLoS One 2018;13(8):e0202039. https://doi.org/10.1371/journal.pone.0202039.
[12] Badawi Y, Ramamoorthy P, Shi H. Hypoxia-inducible factor 1 protects hypoxic astrocytes against glutamate toxicity. ASN Neuro 2012;4(4):231–41. https://doi.org/10.1042/AN20120006.
[13] Choi SH, Bylykbashi E, Chatila ZK, Lee SW, Pulli B, Clemenson GD, et al. Combined adult neurogenesis and BDNF mimic exercise effects on cognition in an Alzheimer's mouse model. Science 2018;361(6406). https://doi.org/10.1126/science.aan8821.

[14] Min JK, Kim JH, Cho YL, Maeng YS, Lee SJ, Pyun BJ, et al. 20(S)-Ginsenoside Rg3 prevents endothelial cell apoptosis via inhibition of a mitochondrial caspase pathway. Biochem Biophys Res Commun 2006;349(3):987–94. https://doi.org/10.1016/j.bbrc.2006.08.129.
[15] Tian J, Fu F, Geng M, Jiang Y, Yang J, Jiang W, et al. Neuroprotective effect of 20(S)-ginsenoside Rg3 on cerebral ischemia in rats. Neurosci Lett 2005;374(2):92–7. https://doi.org/10.1016/j.neulet.2004.10.030.
[16] Chaban Y, Boekema EJ, Dudkina NV. Structures of mitochondrial oxidative phosphorylation supercomplexes and mechanisms for their stabilisation. Biochim Biophys Acta 2014;1837(4):418–26. https://doi.org/10.1016/j.bbabio.2013.10.004.
[17] Schubert D, Soucek T, Blouw B. The induction of HIF-1 reduces astrocyte activation by amyloid beta peptide. Eur J Neurosci 2009;29(7):1323–34. https://doi.org/10.1111/j.1460-9568.2009.06712.x.
[18] Hwang M, Song SH, Chang MS, Koh SH. Glia-like cells from human mesenchymal stem cells protect neural stem cells in an in vitro model of alzheimer's disease by reducing NLRP-3 inflammasome. Dement Neurocogn Disord 2021;20(1):1–8. https://doi.org/10.12779/dnd.2021.20.1.1.
[19] Choi YK, Maki T, Mandeville ET, Koh SH, Hayakawa K, Arai K, et al. Dual effects of carbon monoxide on pericytes and neurogenesis in traumatic brain injury. Nat Med 2016;22(11):1335–41. https://doi.org/10.1038/nm.4188.
[20] Tint I, Jean D, Baas PW, Black MM. Doublecortin associates with microtubules preferentially in regions of the axon displaying actin-rich protrusive structures. J Neurosci 2009;29(35):10995–1010. https://doi.org/10.1523/JNEUROSCI.3399-09.
[21] Na HJ, Hwang JY, Lee KS, Choi YK, Choe J, Kim JY, et al. TRAIL negatively regulates VEGF-induced angiogenesis via caspase-8-mediated enzymatic and non-enzymatic functions. Angiogenesis 2014;17(1):179–94. https://doi.org/10.1007/s10456-013-9387-0.
[22] Semenza GL. Life with oxygen. Science 2007;318(5847):62–4.
[23] Choi YK, Kim CK, Lee H, Jeoung D, Ha KS, Kwon YG, et al. Carbon monoxide promotes VEGF expression by increasing HIF-1alpha protein level via two distinct mechanisms, translational activation and stabilization of HIF-1alpha protein. J Biol Chem 2010;285(42):32116–25.
[24] Chan DA, Sutphin PD, Yen SE, Giaccia AJ. Coordinate regulation of the oxygen-dependent degradation domains of hypoxia-inducible factor 1 alpha. Mol Cell Biol 2005;25(15):6415–26. https://doi.org/10.1128/MCB.25.15.6415-6426.
[25] Ivan M, Kondo K, Yang H, Kim W, Valiando J, Ohh M, et al. HIFalpha targeted for VHL-mediated destruction by proline hydroxylation: implications for O2 sensing. Science 2001;292(5516):464–8.
[26] Arenberg DA, Keane MP, DiGiovine B, Kunkel SL, Morris SB, Xue YY, et al. Epithelial-neutrophil activating peptide (ENA-78) is an important angiogenic factor in non-small cell lung cancer. J Clin Invest 1998;102(3):465–72. https://doi.org/10.1172/JCI3145.
[27] Caunt M, Hu L, Tang T, Brooks PC, Ibrahim S, Karpatkin S. Growth-regulated oncogene is pivotal in thrombin-induced angiogenesis. Cancer Res 2006;66(8):4125–32. https://doi.org/10.1158/0008-5472.CAN-05-2570.
[28] Chen Y, Zhong M, Liang L, Gu F, Peng H. Interleukin-17 induces angiogenesis in human choroidal endothelial cells in vitro. Invest Ophthalmol Vis Sci 2014;55(10):6968–75. https://doi.org/10.1167/iovs.14-15029.
[29] Enzmann V, Lecaude S, Kruschinski A, Vater A. CXCL12/SDF-1-Dependent retinal migration of endogenous bone marrow-derived stem cells improves visual function after pharmacologically induced retinal degeneration. Stem Cell Rev 2017;13(2):278–86. https://doi.org/10.1007/s12015-016-9706-0.
[30] Sun Y, Jin K, Xie L, Childs J, Mao XO, Logvinova A, et al. VEGF-induced neuroprotection, neurogenesis, and angiogenesis after focal cerebral ischemia. J Clin Invest 2003;111(12):1843–51. https://doi.org/10.1172/JCI17977.
[31] During MJ, Cao L. VEGF, a mediator of the effect of experience on hippocampal neurogenesis. Curr Alzheimer Res 2006;3(1):29–33.
[32] Cheng X, Wang H, Zhang X, Zhao S, Zhou Z, Mu X, et al. The role of SDF-1/CXCR4/CXCR7 in neuronal regeneration after cerebral ischemia. Front Neurosci 2017;11:590. https://doi.org/10.3389/fnins.2017.00590.
[33] Lin Y, Zhang JC, Yao CY, Wu Y, Abdelgawad AF, Yao SL, et al. Critical role of astrocytic interleukin-17 A in post-stroke survival and neuronal differentiation of neural precursor cells in adult mice. Cell Death Dis 2016;7(6):e2273. https://doi.org/10.1038/cddis.2015.284.
[34] Braun SM, Jessberger S. Adult neurogenesis and its role in neuropsychiatric disease, brain repair and normal brain function. Neuropathol Appl Neurobiol 2014;40(1):3–12. https://doi.org/10.1111/nan.12107.